



Article

Throughput Analysis of Buffer-Aided Decode-and-Forward Wireless Relaying with RF Energy Harvesting

Phat Huynh ^{1,*}, Khoa T Phan ², Bo Liu ³ and Robert Ross ¹

¹ Department of Engineering, La Trobe University, Bundoora 3086, Australia; R.Ross@latrobe.edu.au

² Department of Computer Science and Information Technology, La Trobe University, Bundoora 3086, Australia; K.Phan@latrobe.edu.au

³ School of Computer Science, University of Technology Sydney, Ultimo 2007, Australia; Bo.Liu@uts.edu.au

* Correspondence: Tommy.Huynh@latrobe.edu.au

Received: 10 January 2020; Accepted: 20 February 2020; Published: 23 February 2020

Abstract: In this paper, we investigated a buffer-aided decode-and-forward (DF) wireless relaying system over fading channels, where the source and relay harvest radio-frequency (RF) energy from a power station for data transmissions. We derived exact expressions for end-to-end throughput considering half-duplex (HD) and full-duplex (FD) relaying schemes. The numerical results illustrate the throughput and energy efficiencies of the relaying schemes under different self-interference (SI) cancellation levels and relay deployment locations. It was demonstrated that throughput-optimal relaying is not necessarily energy efficiency-optimal. The results provide guidance on optimal relaying network deployment and operation under different performance criteria.

Keywords: vehicular communication; green communication; energy harvesting; buffer-aided relaying

1. Introduction

Internet of things (IoT) is a major technology of the incoming industrial revolution 4.0 [1]. An IoT network consist of a large number of connected devices, each of which requires a reliable energy supply for efficient operation [2]. This requirement can be satisfied by embedding batteries into the IoT devices, possibly incurring high-cost and safety-related issues to replace [3]. Harvesting energy from the ambient environment, such as solar, wind, thermal and radio frequency (RF) signals to empower electronic devices is becoming the future of IoT [4]. In particular, energy harvesting (EH) from RF signals has attracted significant interest because it can offer simultaneous wireless information and power transfer (SWIPT) while other natural energy sources are usually reliant on the climate of deployment locations [5–7]. Such SWIPT-based systems are inherently useful in applications with hard-to-access devices such as inside bodies, building structures, vehicles, or remote areas [8]. In particular, EH-based communications systems are suitable for intelligent transportation systems (ITS) [9–11], where vehicles form a vehicle-to-vehicle (V2V) wireless communication network. This V2V communication can take place in transit with moving transmitters and receivers, as well as in slow-changing environments such as car parks, where the devices are more static. Moreover, full-duplex communication is a mature field in wireless communication. There have been numerous works in the literature on the combination of energy harvesting and full-duplex for more advanced and self-sustain communication [12,13].

In this paper, we studied a buffer-aided dual-hop wireless relaying communication model, where the source and relay harvest RF energy from a dedicated power station for data transmission to the destination.

Our model represents a simple yet powerful EH-based system where all the communication devices are energy self-sufficient by harvesting RF energy. Along this line of research, existing literature has proposed and analyzed several wireless relaying models using RF energy harvesting. For example, in [5] and [6], the relay harvests RF energy from the source, which has access to a reliable power source. The work [7] alternatively considers that the source harvests energy from the relay. The authors investigated two cases: without battery storage and with unlimited battery capacity. In contrast, our work has both the source and the relay as EH-based nodes. While such an assumption has been considered in [14,15], our work considers a data buffer at the relay for (end-to-end) throughput enhancement with both half-duplex (HD) and full-duplex (FD) relaying modes. In [16], the authors developed an efficient wireless energy transfer (WET) policy for a multiple-node communication network that is powered by a single energy access point (E-AP). This work focuses on the resource allocation for a network where communications between nodes are direct transmissions. In reality, direct transmissions often encounter challenges in extended distances due to hostility on the channel. Our paper considers a wireless buffer-aided relaying communication scheme that is particularly useful to ensure quality-of-service (QoS) in a long transmission range. Overall, the main contributions of our work can be summarized as follows:

(1) We derive analytical throughput expressions in buffer-aided decode-and-forward HD and FD relaying modes. The expressions also take into account the fading channel statistics, EH and data transmission duration, as well as the self-interference (SI) cancellation level (for FD relaying). These expressions can be exploited to determine the parameters for optimal throughput performance.

(2) In addition to the throughput, we also investigate the energy efficiency of the relaying schemes. This performance benchmark is particularly relevant for green V2V communication applications.

(3) We perform numerical simulations to demonstrate the throughput and energy efficiency performance of the relaying schemes under different SI cancellation levels and relay locations. The results showed that with sufficiently small residual SI, FD relaying achieves higher throughput and energy efficiency than HD relaying. Moreover, it is revealed that throughput-optimal relaying is not necessarily energy efficiency-optimal in general. The results provide guidance on optimal relaying network deployment and operation under different performance criteria.

2. System Model and Throughput Analysis

2.1. System Model

The source node, **S** and the relay, **R** harvest energy from the power station, **P** for data transmission from **S** to **D** (Figure 1). We assume that **R** only harvest energy from **P** and does not perform self-energy recycling from its own transmission energy. The complex channel coefficients on the **SR**, **RD**, **PS** and **PR** channels are denoted by h_1 , h_2 , h_3 and h_4 respectively. d_1 , d_2 , d_3 and d_4 denote the distances of the communication channels corresponding with their channel coefficient notations. The angle between the **SP** and **PD** channels is denoted by θ . Figure 2 illustrates the time allocations in a transmission block in HD and FD relaying modes. The block time T is the total time for EH and information transmissions from **S** to **D** via the relay. For simplicity, it is assumed that the fading-block duration equals to T within which the channel coefficients remain constant and vary independently over fading blocks. α_1 indicates the harvesting time. In the HD mode, the data transmission time is divided into two parts α_2 and α_3 for information transmission time on **SR** and **RD** channels, respectively. In contrast, FD communication features simultaneous data reception and transmission at the relay; hence, the time allocated for these two transmissions is simply $1 - \alpha_1$.

We can see that for a given α_1 , when α_2 increases, the throughput on the **SR** channel increases, but it suppresses the throughput on the **RD** channels, and vice versa. Hence, optimal values of α_2 and α_3

respectively equalize the throughput on the **SR** and **RD** channels. The process to determine optimal α_2 and α_3 is illustrated in Figure 3.

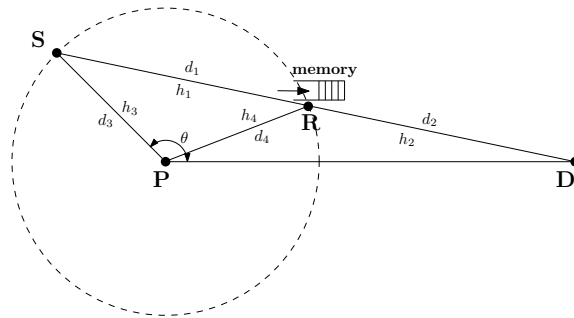


Figure 1. A wireless communication system consists of energy-constrained source and relay.

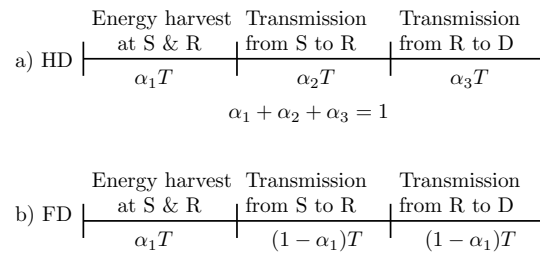


Figure 2. Time allocation in a transmission block: (a) Half duplex, (b) Full duplex.

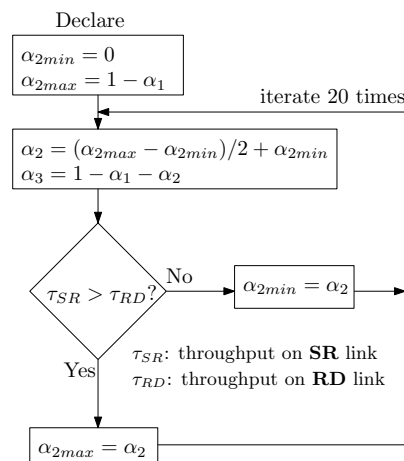


Figure 3. Process to determine optimal α_2 and α_3 values.

The energy harvested at **S** and **R** is given by:

$$E_s = \eta P |h_3|^2 \alpha_1 T, \quad E_r = \eta P |h_4|^2 \alpha_1 T \tag{1}$$

where $0 < \eta < 1$ is the energy conversion efficiency of energy harvesting circuitry at **S** and **R**, P is the RF signal power broadcast by the power source. The channel power gains are computed using the standard path loss model:

$$|h_p|^2 = \left(\frac{c}{4\pi f_c} \right)^2 d_p^{-m} e_p = F d_p^{-m} e_p, \quad p \in \{1, 2, 3, 4\} \quad (2)$$

where $F \triangleq \left(\frac{c}{4\pi f_c} \right)^2$, c is the speed of light, f_c is the carrier frequency, m is the path loss exponent. Rayleigh fading channels are assumed because we consider a general deployment in reality where the channels between the power station and the devices are multi-paths. As a result, e_p is a complex exponential random variable with unit mean.

2.2. Half-Duplex (HD) Relaying

We first consider HD relaying. The transmission powers $P_{s,HD}$ of **S** and $P_{r,HD}$ of **R** are given by:

$$P_{s,HD} = \frac{E_s}{\alpha_2 T} = \frac{\eta P |h_3|^2 \alpha_1}{\alpha_2}, \quad P_{r,HD} = \frac{E_r}{\alpha_3 T} = \frac{\eta P |h_4|^2 \alpha_1}{\alpha_3}. \quad (3)$$

The signal-to-noise ratios (SNR) at the relay, $\gamma_{r,HD}$, and at the destination, $\gamma_{d,HD}$ are given by:

$$\gamma_{r,HD} = \frac{\eta P |h_1|^2 |h_3|^2 \alpha_1}{\alpha_2 \sigma_{sr}^2}, \quad \gamma_{d,HD} = \frac{\eta P |h_2|^2 |h_4|^2 \alpha_1}{\alpha_3 \sigma_{rd}^2}. \quad (4)$$

where σ_{sr}^2 and σ_{rd}^2 are variances of the AWGN noise at the relay and destination, respectively.

With a buffer-aided relay system, the (end-to-end) throughput τ_{HD} is given by [17]:

$$\begin{aligned} \tau_{HD} &= \min\{\mathbb{E}[\alpha_2 \log_2(1 + \gamma_{r,HD})], \mathbb{E}[\alpha_3 \log_2(1 + \gamma_{d,HD})]\} \\ &= \min\{\alpha_2 C_{r,HD}, \alpha_3 C_{d,HD}\} \end{aligned} \quad (5)$$

where $C_{r,HD}$ and $C_{d,HD}$ are the ergodic capacities of the **SR** and the **RD** channels, respectively. $\mathbb{E}[\cdot]$ denotes the statistical expectation over fading channels. We also assumed the timescales of energy harvesting and channel fading block duration is sufficiently long so that long codeword transmissions are possible to achieve the capacity. In the case of short packets (or finite blocklength code) [18], only smaller rates than the capacity $\log(1 + \text{SNR})$ are achieved and hence, the throughput obtained in our work will serve as the upper bounds. If the system were using non-buffer relaying mode, the throughput would be given by:

$$\mathbb{E}[\min\{\alpha_2 \log_2(1 + \gamma_{r,HD}), \alpha_3 \log_2(1 + \gamma_{r,HD})\}]. \quad (6)$$

Mathematically, we can see that the throughput of a buffer-aid system is always higher than a non-buffer one [17].

In order to find the analytical expression for $C_{r,HD}$, we firstly evaluate the cumulative distribution function (CDF) of $\gamma_{r,HD}$, $F_{\gamma_{r,HD}}(\gamma)$ and then evaluate the probability distribution function (PDF) of $\gamma_{r,HD}$, $f_{\gamma_{r,HD}}(\gamma)$. The CDF $F_{\gamma_{r,HD}}(\gamma)$ is given by:

$$F_{\gamma_{r,HD}} = \Pr(\gamma_{r,HD} < \gamma) = 1 - t_1 K_1(t_1) \quad (7)$$

where $\Pr(\cdot)$ denotes probability operator, $K_1(\cdot)$ is the first-order of the second kind modified Bessel function, $t_1 = \sqrt{\frac{4b_1\gamma}{\lambda_1\lambda_3}}$, $b_1 = \frac{\alpha_2\sigma_{sr}^2}{\eta P \alpha_1 F^2 d_1^{-m} d_2^{-m}}$ and λ_1 and λ_3 are the mean values of the exponential random

variables $|h_1|^2$ and $|h_3|^2$, respectively.

Proof. Appendix A

The PDF $f_{\gamma_{r,HD}}(\gamma)$ is then given by (using [19], 8.486.18):

$$\begin{aligned} f_{\gamma_{r,HD}}(\gamma) &= \frac{\partial(F_{\gamma_{r,HD}})}{\partial\gamma} \\ &= t_1 K_0(t_1) t_1' \\ &= \frac{2b_1}{\lambda_1 \lambda_3} K_0(t_1). \end{aligned} \quad (8)$$

The capacity of the **SR** channel, $C_{r,HD}$ is:

$$\begin{aligned} C_{r,HD} &= \int_0^\infty f_{\gamma_{r,HD}}(\gamma) \log_2(1 + \gamma) d\gamma \\ &= \int_0^\infty \frac{2b_1}{\lambda_1 \lambda_3} K_0(t_1) \log_2(1 + \gamma) d\gamma. \end{aligned} \quad (9)$$

Similarly, the capacity of the **RD** channel, $C_{d,HD}$ can be implied as:

$$C_{d,HD} = \int_0^\infty \frac{2b_2}{\lambda_2 \lambda_4} K_0(t_2) \log_2(1 + \gamma) d\gamma \quad (10)$$

where $t_2 = \sqrt{\frac{4b_2\gamma}{\lambda_2\lambda_4}}$, $b_2 = \frac{\alpha_3\sigma_{rd}^2}{\eta P\alpha_1 F^2 d_2^{-m} d_4^{-m}}$ and λ_2 and λ_4 are the mean values of the exponential random variables $|h_2|^2$ and $|h_4|^2$, respectively. \square

2.3. Full-Duplex (FD) Relaying

We now consider FD relaying. The transmission powers $P_{s,FD}$ and $P_{r,FD}$ in FD communication, are given by:

$$P_{s,FD} = \frac{E_s}{(1 - \alpha_1)T}, \quad P_{r,FD} = \frac{E_r}{(1 - \alpha_1)T}. \quad (11)$$

Under FD relaying, data reception at the relay suffers SI generated by the its own transmission signal, in addition to the AWGN noise.

The capacity of the **RD** channel, $C_{d,FD}$ is analogous to the case of HD relaying:

$$C_{d,FD} = \int_0^\infty \frac{2b_3}{\lambda_2 \lambda_4} K_0(t_3) \log_2(1 + \gamma) d\gamma \quad (12)$$

where $t_3 = \sqrt{\frac{4b_3\gamma}{\lambda_2\lambda_4}}$ and $b_3 = \frac{(1-\alpha_1)\sigma_{rd}^2}{\eta P\alpha_1 F^2 d_2^{-m} d_4^{-m}}$. On the other hand, the SNR of the **SR** link, $\gamma_{r,FD}$, is given by:

$$\gamma_{r,FD} = \frac{P_{s,FD}|h_1|^2}{\beta P_{r,FD} + \sigma_{sr}^2} = \frac{\eta P|h_1|^2|h_3|^2\alpha_1}{\eta P\beta|h_4|^2\alpha_1 + (1 - \alpha_1)\sigma_{sr}^2} \quad (13)$$

where β is the residual SI noise factor. The CDF of $\gamma_{r,FD}$, $F_{\gamma_{r,FD}}(\gamma)$ is given by:

$$F_{\gamma_{r,FD}}(\gamma) = 1 - \frac{1}{\lambda_4} \int_0^\infty e^{-z/\lambda_4} t_4 K_1(t_4) dz \quad (14)$$

where $t_4 = \sqrt{\frac{4\gamma(b_4z+c_4)}{a_4\lambda_1\lambda_3}}$, $a_4 = \eta P\alpha_1 F^2 d_1^{-m} d_3^{-m}$, $c_4 = (1 - \alpha_1)\sigma_{sr}^2$ and $b_4 = \eta P\beta\alpha_1 F d_4^{-m}$.

Proof. Appendix B

The PDF of $\gamma_{r,FD}$, $f_{\gamma_{r,FD}}(\gamma)$ is then given by:

$$\begin{aligned} f_{\gamma_{r,FD}}(\gamma) &= \frac{\partial F_{\gamma_{r,FD}}(\gamma)}{\partial \gamma} \\ &= \frac{1}{\lambda_4} \int_0^\infty e^{-\frac{z}{\lambda_4}} t_4 K_0(t_4) t_4' dz \quad (\text{Using Leibniz's rule}) \\ &= \frac{2}{\lambda_1 \lambda_3 \lambda_4} \int_0^\infty e^{-\frac{z}{\lambda_4}} K_0(t_4) \frac{b_4 z + c_4}{a_4} dz. \end{aligned} \quad (15)$$

The capacity of the RD channel is then given by:

$$C_{r,FD} = \frac{2}{\lambda_1 \lambda_3 \lambda_4} \int_0^\infty \int_0^\infty e^{-\frac{z}{\lambda_4}} K_0(t_4) \frac{b_4 z + c_4}{a_4} \log(1 + \gamma) dz d\gamma. \quad (16)$$

Finally, the throughput τ_{FD} is given by:

$$\tau_{FD} = (1 - \alpha_1) \cdot \min\{C_{r,FD}, C_{d,FD}\}. \quad (17)$$

□

Table 1 below summarizes the analytical expressions of ergodic capacities and end-to-end throughput in HD and FD transmission modes.

Table 1. Summarized analytical expressions of ergodic capacities and end-to-end throughput.

Half-Duplex (HD)	Full-Duplex (FD)
Ergodic Capacity of SR channel	
$C_{r,HD} = \int_0^\infty \frac{2b_1}{\lambda_1 \lambda_3} K_0(t_1) \log_2(1 + \gamma) d\gamma \quad (18)$	$C_{r,FD} = \frac{2}{\lambda_1 \lambda_3 \lambda_4} \int_0^\infty \int_0^\infty e^{-z/\lambda_4} K_0(t_4) \frac{b_4 z + c_4}{a_4} \log_2(1 + \gamma) dz d\gamma \quad (19)$
where, $t_1 = \sqrt{\frac{4b_1\gamma}{\lambda_1\lambda_3}}$, $b_1 = \frac{\alpha_2\sigma_{sr}^2}{\eta P\alpha_1 F^2 d_1^{-m} d_2^{-m}}$	where, $t_4 = \sqrt{\frac{4\gamma(b_4z+c_4)}{a_4\lambda_1\lambda_3}}$, $a_4 = \eta P\alpha_1 F^2 d_1^{-m} d_3^{-m}$, $b_4 = \eta P\beta\alpha_1 F d_4^{-m}$, $c_4 = (1 - \alpha_1)\sigma_{sr}^2$
Ergodic Capacity of RD channel	
$C_{d,HD} = \int_0^\infty \frac{2b_2}{\lambda_2 \lambda_4} K_0(t_2) \log_2(1 + \gamma) d\gamma \quad (20)$	$C_{d,FD} = \int_0^\infty \frac{2b_3}{\lambda_2 \lambda_4} K_0(t_3) \log_2(1 + \gamma) d\gamma F \quad (21)$
where, $t_2 = \sqrt{\frac{4b_2\gamma}{\lambda_2\lambda_4}}$, $b_2 = \frac{\alpha_3\sigma_{rd}^2}{\eta P\alpha_1 F^2 d_2^{-m} d_4^{-m}}$	where, $t_3 = \sqrt{\frac{4b_3\gamma}{\lambda_2\lambda_4}}$, $b_3 = \frac{(1-\alpha_1)\sigma_{rd}^2}{\eta P\alpha_1 F^2 d_2^{-m} d_4^{-m}}$
End-to-end throughput	
$\tau_{HD} = \min\{\alpha_2 C_{r,HD}, \alpha_3 C_{d,HD}\} \quad (22)$	$\tau_{FD} = (1 - \alpha_1) \cdot \min\{C_{r,FD}, C_{d,FD}\} \quad (23)$

3. Numerical Results and Discussion

3.1. Simulation Parameters

In our experiments, Matlab was used as the simulation tool because it contains efficient built-in functions to simplify the coding and accelerate the simulation speed. The geometrical settings of the model simulates a wireless V2V communication system in constrained environments such as car parks where transmitters and receivers are more static or slowly moving. We assume that the dedicated power station has an effective range of 10 m, or $d_3 = 10$ m. The distance between the power station and the destination is 30 m. The angle $\theta = 135^\circ$, using geometry we can compute the **SD** distance (i.e., $d_1 + d_2$) and maximum d_1 as 37.74 m and 16 m respectively. In the simulations, the distance d_1 is varied from 1 to the maximum d_1 with an increment of 1 m. We compute the d_2 and d_4 adaptively with each value of d_1 using geometry.

In the simulations, we compute the channel gains using the standard path loss model with carrier frequency $f_c = 2.4$ GHz and path loss exponent $m = 2.7$. Moreover, we assume that the noise power per Hertz is -160 dBm, or -190 dB, giving the total noise power is $10^{-19} \times 100$ kHz (transmitted bandwidth) = 10^{-14} .

We assume that the energy harvesting circuitry at **S** and **R** ideally has maximum efficiency, $\eta = 1$. The transmitted power at the power station, P is set at 10 Watts and the SINR varies in a range $[-\infty -10\text{dB}]$. The mean values, $\lambda_1, \lambda_2, \lambda_3$ and λ_4 are all set to 1.

Our model considers imperfect SI cancellation in FD communication with the residual SI is proportional to the relay transmission power. The calculation of SINR is given by:

$$\text{SINR} = \frac{\beta P_{r,FD}}{\text{Total noise power}} = \frac{\beta P_{r,FD}}{10^{-14}}. \quad (24)$$

The energy efficiency η_{EE} is defined as the number of bits transmitted by one Joules:

$$\eta_{EE} = \frac{\tau}{P\alpha_1 T + E_{CC}} \quad (25)$$

where E_{CC} is the circuitry energy consumption and it is set at 1.5 WT.

3.2. Effects of Energy Harvesting Time

To investigate the effects of the energy harvesting time factor α_1 on the throughput performance of HD and FD communications, we fix the relay location at $d_1 = 9$ m.

Figure 4 shows that the throughput increases when α_1 increases from 0 to an optimal value and starts decreasing beyond the optimal value of α_1 . This can be explained as smaller α_1 values give less time for energy harvesting, causing less energy for transmission and a lower end-to-end throughput as a result. On the other hand, when α_1 is beyond the optimal value, more time is spent for energy harvesting, but time for data transmission is constrained. Hence, it also leads to a lower throughput value.

Figure 4 also demonstrates that the optimal harvesting time increases when SINR decreases in FD mode. This is because lower SINR values impose slower increase of SI when the relay is harvesting more energy.

For a given α_1 value, FD communication always has higher effective transmission time compared to HD. However, the transmission time advantage is not sufficient to compensate for the throughput loss caused by the SI trade-off. Therefore, in our simulations, HD mode only produces lower throughput than the no-SI FD communication as shown in Figure 4.

Figure 5 reveals that energy efficiency increases when α_1 increases from 0 to an optimal value and starts decreasing beyond the optimal α_1 value. At smaller α_1 values, the harvested energy is insignificant compared to the E_{CC} , causing lower energy efficiencies. Although larger α_1 (i.e., beyond the optimal value) generate more harvested energy, it constrains the data transmission capacity and reduces the energy efficiency as a result.

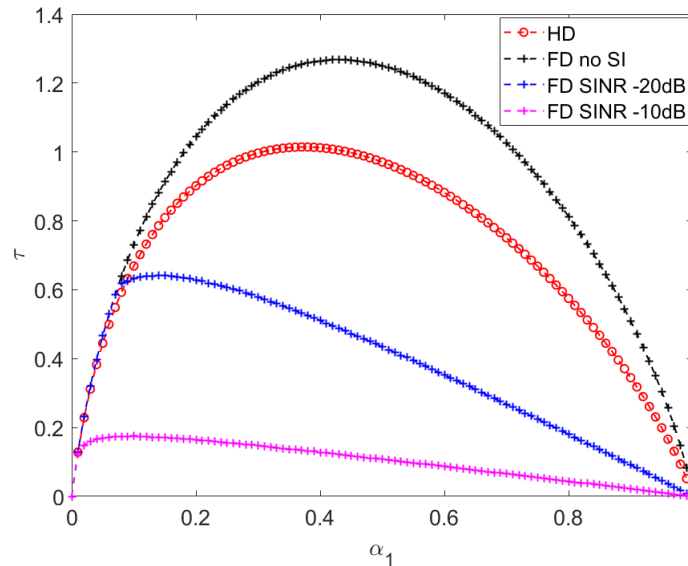


Figure 4. End-to-end throughput τ vs. harvesting time factor α_1 with $d_1 = 9$, $d_3 = 10$, $P = 10$.

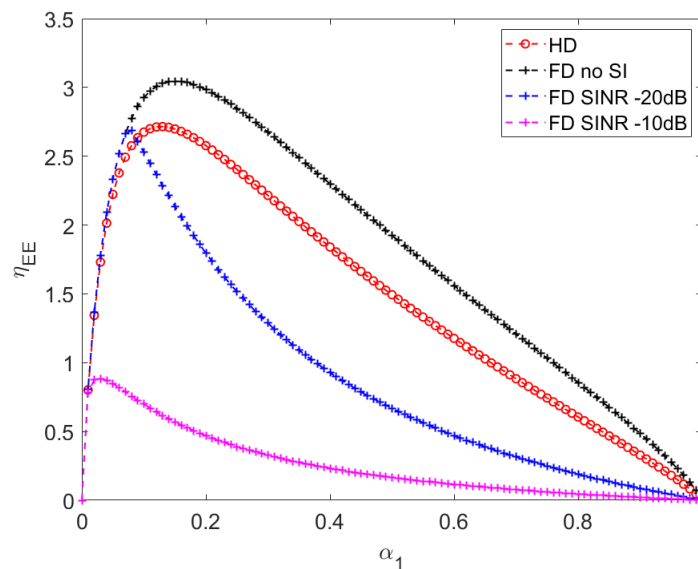


Figure 5. Energy efficiency η_{EE} vs. harvesting time factor α_1 with $d_1 = 9$, $d_3 = 10$, $P = 10$.

3.3. Effects of Relay Location

In general, the maximum throughput improves when the relay moves from the source toward an optimal location and starts decreasing beyond that point. It can be observed that HD communication and

FD communication with perfect SI cancellation outperform the others, particularly when d_1 is further from **S** (i.e. $> 50\%$ **SR** length).

Additionally, HD and no-SI FD communication have optimal relay locations within the range of 6–10 m ($\pm 10\%$ from the middle point of **SR**). The distance from the relay to the power station is shortest when the relay is at the middle of **SR**. Around this point, more harvested energy favors HD and no-SI FD communication.

In contrast, higher SINR FD communication (i.e., ≥ -20 dB) has optimal relay locations closer to the source. After the end-to-end throughput achieves the peak, it plunges rapidly before it marginally decreases to a stable value. When d_1 increases from 1 to an optimal value, the relay harvests more energy for transmission, improving the end-to-end throughput. In this stage, the end-to-end throughput increase is driven by the capacity increase on the **RD** channel.

When SINR level is high, SI is quickly amplified as d_1 moves from the optimal locations to the middle point of **SR** due to the larger energy harvested by the relay, hence rapidly reduces the throughput on the **SR** channel. Beyond the middle point of **SR**, larger source-relay distance reduces the channel gain due to higher path loss, resulting in lower channel capacity on the **SR** link. Beyond the optimal relay location, the decline of the end-to-end throughput is dictated by the capacity reduction on the **SR** link.

Figure 6 suggests that in applications where energy efficiency is important (i.e., green communication), HD and no-SI FD communication offer highest achievable energy efficiencies in the range 6–10 m of d_1 . This is consistent with results achieved in Figure 7. It leads to a result that highest end-to-end throughput with highest energy efficiency can be achieved within $\pm 10\%$ range from the middle point of the **SR** distance, using HD communication or FD with perfect SI cancellation. Nevertheless, HD communication can be more suitable in particular applications that tolerate certain throughput and efficiency performance, because it requires less implementation complexity than FD communication.

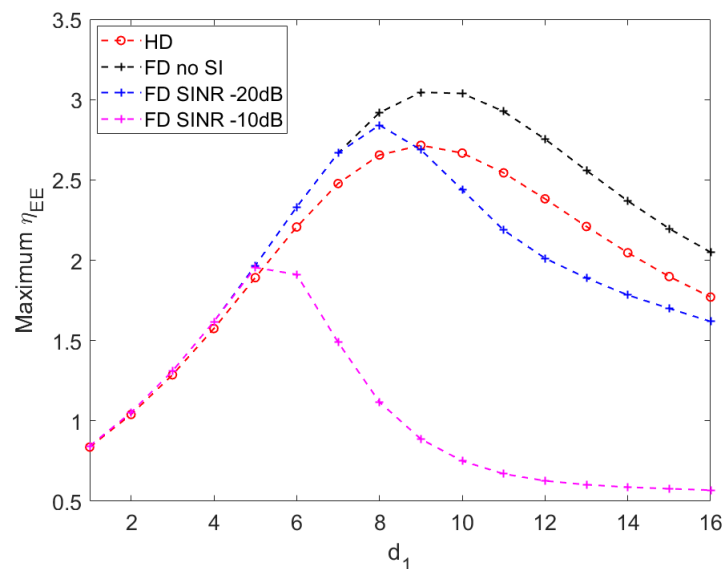


Figure 6. Maximum energy efficiency vs. distance from source to relay d_1 with $d_3 = 10$, $P = 10$.

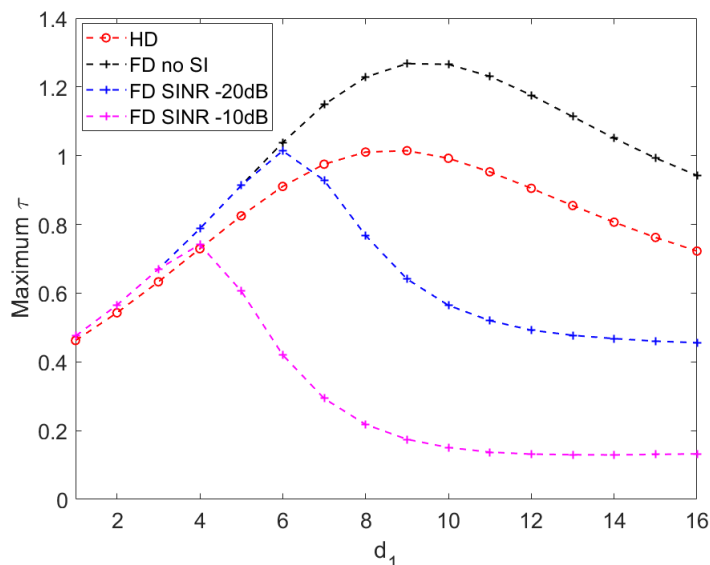


Figure 7. Maximum throughput vs. distance from source to relay d_1 with $d_3 = 10$, $P = 10$.

4. Conclusions

In this paper, a buffer-aided DF relaying model for V2V communication was investigated, which consists of energy-constrained source and relay harvest RF energy from a dedicated power station for data processing and transmission. The numerical results compare the throughput performance and the energy efficiency between HD and FD communications under the effects of the energy harvesting time and the relay deployment locations. To compute the throughput, we derived ergodic capacity expressions which are summarized in Table 1. The work in this paper can be extended by applying resource allocation techniques [17] and investigating a constrained delay at the relay [20]. In the future, we will also investigate the combination of energy harvesting with more complicated non-orthogonal multiple access (NOMA) or multi-point NOMA cooperative relay with various relaying protocols, as an extension of this work [21].

Author Contributions: Conceptualization, P.H. and K.T.P.; Methodology, P.H. and K.T.P.; formal analysis, P.H.; investigation, P.H.; writing original draft, P.H.; review and editing, K.T.P., B.L. and R.R.; supervision, K.T.P. All authors have read and agreed to the published version of the manuscript.

Funding: La Trobe University star-up grant. Grant number: 3.2501.13.51.

Acknowledgments: We would like to thank La Trobe University, Australia for providing funding support for this research.

Conflicts of Interest: The authors declare no conflict of interest.

Appendix A

This appendix presents the working details to derive the CDF $F_{\gamma_{r,HD}}(\gamma)$ of $\gamma_{r,HD}$ in HD communication.

$$\begin{aligned}
 F_{\gamma_{r,HD}}(\gamma) &= \Pr(\gamma_{r,HD} < \gamma) \\
 &= \Pr\left(\frac{\eta P \alpha_1 |h_1|^2 |h_3|^2}{\alpha_2 \sigma_{sr}^2} < \gamma\right) \\
 &= \Pr\left(e_1 < \frac{b_1 \gamma}{e_3}\right) \quad \text{where } b_1 = \frac{\alpha_2 \sigma_{sr}^2}{\eta P \alpha_1 F^2 d_1^{-m} d_3^{-m}} \\
 &= \int_0^\infty f_{e_3}(x) \left(1 - e^{-\frac{b_1 \gamma}{\lambda_1 x}}\right) dx \\
 &= \int_0^\infty f_{e_3}(x) dx - \frac{1}{\lambda_3} \int_0^\infty e^{-\frac{x}{\lambda_3} - \frac{b_1 \gamma}{\lambda_1 x}} dx \\
 &= 1 - t_1 K_1(t_1)
 \end{aligned}$$

where $t_1 = \sqrt{\frac{4b_1 \gamma}{\lambda_1 \lambda_3}}$ and $K_1(\cdot)$ is the first order of modified Bessel function of the second kind, using (3.324.1, 518) [19].

Appendix B

This appendix presents the working details to derive the CDF, $F_{\gamma_{r,FD}}$, of $\gamma_{r,FD}$ in FD communication.

$$\begin{aligned}
 F_{\gamma_{r,FD}}(\gamma) &= \Pr(\gamma_{r,FD} < \gamma) \\
 &= \Pr\left(\frac{\eta P \alpha_1 |h_1|^2 |h_3|^2}{\eta P \beta \alpha_1 |h_4|^2 + (1 - \alpha_1) \sigma_{sr}^2} < \gamma\right) \\
 &= \Pr\left(\frac{a_4 e_1 e_3}{b_4 e_4 + c_4} < \gamma\right)
 \end{aligned} \tag{A1}$$

where, $a_4 = \eta P \alpha_1 F^2 d_1^{-m} d_3^{-m}$, $b_4 = \eta P \beta \alpha_1 F d_4^{-m}$, $c_4 = (1 - \alpha_1) \sigma_{sr}^2$.
 $F_{\gamma_{r,FD}}$ is then given by:

$$\begin{aligned}
 F_{\gamma_{r,FD}}(\gamma) &= \Pr\left(e_1 \cdot e_3 < \frac{\gamma(b_4 e_4 + c_4)}{a_4}\right) \\
 &= \int_0^\infty f_{e_4}(z) F_{e_1 \cdot e_3}\left(\frac{\gamma b_4}{a_4} z + \frac{\gamma c_4}{a_4}\right) dz \\
 &= \int_0^\infty \int_0^\infty \int_0^\omega f_{e_4}(z) f_{e_1}(x) f_{e_3}(y) dy dx dz
 \end{aligned} \tag{A2}$$

where $\omega = \frac{\gamma(b_4 z + c_4)}{a_4 x}$ (using the product distribution rule). Because e_1 , e_3 and e_4 are exponential random variables, $F_{\gamma_{r,FD}}$ is then given by:

$$\begin{aligned}
F_{\gamma_{r,FD}}(\gamma) &= \frac{1}{\lambda_1 \lambda_3 \lambda_4} \int_0^\infty \int_0^\infty \int_0^\omega e^{-\frac{z}{\lambda_4}} e^{-\frac{x}{\lambda_1}} e^{-\frac{y}{\lambda_3}} dy dx dz \\
&= -\frac{1}{\lambda_1 \lambda_4} \int_0^\infty \int_0^\infty e^{-\frac{z}{\lambda_4}} e^{-\frac{x}{\lambda_1}} \left[e^{-\frac{\gamma(b_4 z + c_4)}{\lambda_3 a_4 x}} - 1 \right] dx dz \\
&= -\frac{1}{\lambda_4} \int_0^\infty e^{-\frac{z}{\lambda_4}} [t_4 K_1(t_4) - 1] dz \\
&= 1 - \frac{1}{\lambda_4} \int_0^\infty e^{-\frac{z}{\lambda_4}} t_4 K_1(t_4) dz
\end{aligned} \tag{A3}$$

where $t_4 = \sqrt{\frac{4\gamma(b_4 z + c_4)}{a_4 \lambda_1 \lambda_3}}$, using (3.324.1, 518) [19].

References

- Shrouf, F.; Ordieres, J.; Miragliotta, G. Smart factories in Industry 4.0: A review of the concept and of energy management approached in production based on the Internet of Things paradigm. In Proceedings of the 2014 IEEE international conference on industrial engineering and engineering management, Bandar Sunway, Malaysia, 9–12 December 2014; pp. 697–701.
- Li, S.; Da Xu, L.; Zhao, S. The internet of things: A survey. *Inf. Syst. Front.* **2015**, *17*, 243–259. [\[CrossRef\]](#)
- Neethirajan, S. Recent advances in wearable sensors for animal health management. *Sens. Bio-Sens. Res.* **2017**, *12*, 15–29. [\[CrossRef\]](#)
- Atallah, R.; Khabbaz, M.; Assi, C. Energy harvesting in vehicular networks: A contemporary survey. *IEEE Wirel. Commun.* **2016**, *23*, 70–77. [\[CrossRef\]](#)
- Nasir, A.A.; Zhou, X.; Durrani, S.; Kennedy, R.A. Relaying protocols for wireless energy harvesting and information processing. *IEEE Trans. Wirel. Commun.* **2013**, *12*, 3622–3636. [\[CrossRef\]](#)
- Nasir, A.A.; Zhou, X.; Durrani, S.; Kennedy, R.A. Throughput and ergodic capacity of wireless energy harvesting based DF relaying network. In Proceedings of the 2014 IEEE International Conference on Communications (ICC), Sydney, Australia, 10–14 June 2014; pp. 4066–4071.
- Zlatanov, N.; Ng, D.W.K.; Schober, R. Capacity of the two-hop relay channel with wireless energy transfer from relay to source and energy transmission cost. *IEEE Trans. Wireless Commun.* **2017**, *16*, 647–662. [\[CrossRef\]](#)
- Magno, M.; Boyle, D. Wearable energy harvesting: From body to battery. In Proceedings of the 2017 12th International Conference on Design & Technology of Integrated Systems In Nanoscale Era (DTIS), Palma de Mallorca, Spain, 4–6 April 2017; pp. 1–6.
- Ahmed, I.; Phan, K.T.; Le-Ngoc, T. Optimal stochastic power control for energy harvesting systems with delay constraints. *IEEE J. Sel. Areas Commun.* **2016**, *34*, 3512–3527. [\[CrossRef\]](#)
- Campolo, C.; Molinaro, A.; Berthet, A.O.; Vinel, A. Full-duplex radios for vehicular communications. *IEEE Commun. Mag.* **2017**, *55*, 182–189. [\[CrossRef\]](#)
- Naik, G.; Choudhury, B.; Park, J.M. IEEE 802.11 bd & 5G NR V2X: Evolution of Radio Access Technologies for V2X Communications. *IEEE Access* **2019**, *7*, 70169–70184.
- Zeng, Y.; Zhang, R. Full-duplex wireless-powered relay with self-energy recycling. *IEEE Wirel. Commun. Lett.* **2015**, *4*, 201–204. [\[CrossRef\]](#)
- Wang, D.; Zhang, R.; Cheng, X.; Yang, L.; Chen, C. Relay selection in full-duplex energy-harvesting two-way relay networks. *IEEE Trans. Commun. Netw.* **2017**, *1*, 182–191. [\[CrossRef\]](#)
- Gündüz, D.; Devillers, B. Two-hop communication with energy harvesting. In Proceedings of the 2011 4th IEEE International Workshop on Computational Advances in Multi-Sensor Adaptive Processing (CAMSAP), San Juan, Puerto Rico, 13–16 December 2011; pp. 201–204.
- Huang, C.; Zhang, R.; Cui, S. Throughput maximization for the Gaussian relay channel with energy harvesting constraints. *IEEE J. Sel. Areas Commun.* **2013**, *31*, 1469–1479. [\[CrossRef\]](#)

16. Movahednasab, M.; Makki, B.; Omidvar, N.; Pakravan, M.R.; Svensson, T.; Zorzi, M. An Energy-Efficient Controller for Wirelessly-Powered Communication Networks. Available online: <https://arxiv.org/abs/1905.05958> (accessed on 21 February 2020).
17. Phan, K.T.; Le-Ngoc, T.; Le, L.B. Optimal resource allocation for buffer-aided relaying with statistical QoS constraint. *IEEE Trans. Commun.* **2016**, *64*, 959–972. [[CrossRef](#)]
18. Makki, B.; Svensson, T.; Zorzi, M. Wireless energy and information transmission using feedback: Infinite and finite block-length analysis. *IEEE Trans. Commun.* **2016**, *64*, 5304–5318. [[CrossRef](#)]
19. Gradshteyn, I.S.; Ryzhik, I.M. *Table of Integrals, Series, and Products*; Academic Press: San Diego, CA, USA, 2014.
20. Phan, K.T.; Le-Ngoc, T. Power allocation for buffer-aided full-duplex relaying with imperfect self-interference cancelation and statistical delay constraint. *IEEE Access* **2016**, *4*, 3961–3974. [[CrossRef](#)]
21. Yang, Z.; Ding, Z.; Fan, P.; Al-Dhahir, N. The impact of power allocation on cooperative non-orthogonal multiple access networks with SWIPT. *IEEE Trans. Wirel. Commun.* **2017**, *16*, 4332–4343. [[CrossRef](#)]



© 2020 by the authors. Licensee MDPI, Basel, Switzerland. This article is an open access article distributed under the terms and conditions of the Creative Commons Attribution (CC BY) license (<http://creativecommons.org/licenses/by/4.0/>).